Nanotechnology **20** (2009) 495503 (8pp) doi:10.1088/0957-4484/20/49/495503

Thermal gradient induced actuation in double-walled carbon nanotubes

Quan-Wen Hou, Bing-Yang Cao and Zeng-Yuan Guo

Key Laboratory for Thermal Science and Power Engineering of Ministry of Education, Department of Engineering Mechanics, Tsinghua University, Beijing 100084, People's Republic of China

E-mail: caoby@tsinghua.edu.cn

Received 2 October 2009, in final form 26 October 2009
Published 6 November 2009
Online at stacks.iop.org/Nano/20/495503

Abstract

Molecular dynamics simulations are applied to investigate the thermal gradient induced actuation in double-walled carbon nanotubes, where a temperature difference can actuate the relative motion of double-walled carbon nanotubes. The thermal driving force calculated through a stationary scheme is on the order of pico Newtons for a 1 K nm^{-1} temperature gradient. The driving force is approximately proportional to the temperature gradient, but not sensitive to the system temperature. For the outer tube longer than 5 nm, the thermal driving force is nearly constant. For the outer tube shorter than 5 nm, however, the driving force decreases with decreasing tube length. The motion trace is found to depend on both the chirality pair and system temperature. A critical temperature can be defined by the potential barrier perpendicular to the minimum energy track of potential patterns. When the system temperature is higher than the critical temperature, the motion shows random behavior. When the system temperature is lower than the critical temperature, the motion, translational and/or rotational, is confined within the minimum energy track, which is indicative of the feasibility of directional control.

(Some figures in this article are in colour only in the electronic version)

1. Introduction

Since the discovery of carbon nanotubes (CNTs) by Iijima in 1991 [1], the extraordinary electrical, mechanical and thermal properties have attracted much attention due to their promising applications in engineering. Especially, double-walled carbon nanotubes (DWNTs) and multi-walled carbon nanotubes (MWNTs) have been considered as elementary building blocks in modern nanoelectromechanical systems because of their ultralow interlayer friction, excellent wearing qualities and the restricted motions (rotation or translation) [2]. Based on MWNTs and DWNTs, many novel nanodevices have been designed, such as nanoswitches [3], nanobearings [4], nanogears [5] and gigahertz oscillators [6] based on actuation by electrical field [3] or mechanical nanomanipulators [2].

The thermal gradient (temperature difference) has been experimentally demonstrated to be capable of driving solid nanodevices more recently [7]. This new driving mechanism for nanodevices may be promising in the design of novel devices. In addition, the transports of nanoparticles or water droplets through CNTs under thermal gradients have also been reported [8–11]. Shiomi and Maruyama suggested that the water–water intrinsic potential energy played a dominant role in driving the water droplets to move inside CNTs [11]. Schoen *et al* calculated the thermal driving force acting on nanoparticles inside CNTs by using molecular dynamics (MD) simulations [8]. There is, however, limited research about the thermal gradient induced actuation of nanodevices based on DWNTs or MWNTs. Furthermore, the quantitative characterization of the thermal driving force and the adequate understanding of the mechanism will be necessary when thermal gradient induced actuation is applied to design new nanodevices.

In this paper, the molecular dynamics simulation method is used to study the thermal gradient induced actuation of DWNTs. The results show that the thermal gradient (temperature difference) is an effective driving mechanism in DWNTs, and the final velocities of the outer tubes are on the order of 100 m s^{-1}. The driving force induced by the thermal gradient is found to be proportional to the thermal

gradient, but insensitive to the system temperature and the length of the outer tube when the tube is longer than 5 nm. A critical temperature is defined by the potential barrier. When the system temperature is higher than the critical temperature, the motions show random behaviors. When the system temperature is lower than the critical temperature, the motions are confined in specific directions. It indicates that directional control is feasible.

2. Simulation method

The simulated system consists of a short outer tube and a long inner tube, i.e. a DWNT, as shown in figure 1. The two ends of the inner tube are fixed. The regions adjacent to the fixed ends are attached to Nose–Hoover thermostats to be maintained at different temperatures respectively. Actuated by this temperature difference, the outer tube moves along and/or around the inner tube. Such a system has been demonstrated to be able to work by recent experiments [7], which yield a firm engineering background for our MD simulations. The Verlet leap frog scheme [12] is applied to integrate the motion equations with a time step of 2 fs. The system is at first set to the average temperature. Then the thermal transport in the simulation system is established during a run of 200 ps while the outer tube is restricted from moving rotationally and translationally by rescaling the velocities of its atoms. After the restriction is removed, the outer tube moves under the actuation of the inner tube. In our MD simulations, the intrawall C–C bonds are modeled by the bond-order potential developed by Brenner [13]

$$E = \sum_i \sum_{j(>i)} [V_{\mathrm{R}}(r_{ij}) - b_{ij} V_{\mathrm{A}}(r_{ij})], \tag{1}$$

where $V_{\mathrm{R}}(r)$ and $V_{\mathrm{A}}(r)$ denote the pair-additive repulsive and attractive interactions, respectively, and b_{ij} represents a many-body coupling between the bond from atom i to atom j and the local environment. The interwall interactions between the carbon atoms are via the Lennard-Jones potential in the form of

$$V(r) = 4\varepsilon\left[\left(\frac{\sigma}{r}\right)^{12} - \left(\frac{\sigma}{r}\right)^{6}\right], \tag{2}$$

in which $\varepsilon = 2.968$ meV, $\sigma = 0.3407$ nm [14].

To acquire the thermal driving force from a stationary process, we use Galliero's method by which the thermophoretic force of particles in the Lennard-Jones fluid has been studied successfully [15]. An atom of the outer tube is attached to the center of the system $x = 0$ thanks to a harmonic potential with a spring constant $K = 0.032$ N m^{-1}. Then, after a transient process of movement under the thermal gradient, the outer tube is displaced to a new equilibrium position. To reduce the time experienced by the outer tube from the initial position to the new equilibrium position, a damping is attached to the outer tube

$$f_{\mathrm{D}} = -\mu u_{\mathrm{C}}, \tag{3}$$

where μ is the damping coefficient and u_{C} is the velocity of the center of mass (CoM) of the outer tube. In all our simulations, μ varies from 2.83×10^{-15} to 2.26×10^{-14} kg s^{-1} depending on

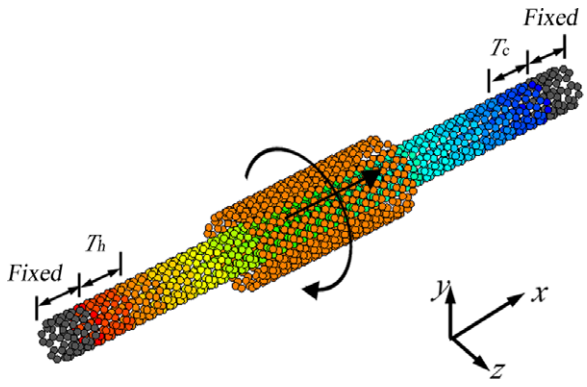

Figure 1. Schematic of the simulated system constructed by a DWNT.

the length of the outer tube. The measure of the displacement of the outer tube from the center of the system, Δx, provides an estimate of the amplitude of the thermal driving force as $F_{\mathrm{T}} = K\Delta x$. For convenience, F_{T} is counted positively though the displacement goes against the thermal gradient. The first 200 ps is used to get a stationary temperature profile in the inner tube. The displacement of the attached atom in the outer tube is recorded for the following 18 ns.

3. Results and discussion

3.1. Thermal gradient actuated motion

We first simulate the thermal gradient driven motion of a (5, 5)@(10, 10) DWNT with various configurations, including different tube lengths (25–50 nm for the inner tube and, 2.5–7.5 nm for the outer tube), average temperatures (500–1100 K) and temperature differences at the two ends of the inner tube (60–800 K). To validate our programs, we calculate the thermal conductivity of the inner tube as a reference. The thermal conductivity of a 7.5 nm long (5, 5) CNT is about 170 W (m K)$^{-1}$ at 500 K and 210 W (m K)$^{-1}$ at 300 K, which is in agreement with the calculated results by Maruyama [16], about 200 W (m K)$^{-1}$ for a (5, 5) CNT with the same length at room temperature. The simulated thermal conductivity is much lower than that measured by Pop *et al* [17] at 500 K because the short tube length in our simulations increases the phonon boundary scattering and confines the thermal conductivity. In all our simulations, the outer tube moves toward the cold end of the inner tube, no matter what the thermal gradient direction is. It indicates that the thermal gradient can be used to actuate the relative motion in DWNTs.

Let us look at a typical simulation in which the lengths of the inner tube and the outer tube are 50 nm (4000 atoms) and 7.5 nm (1200 atoms), respectively, and the average system temperature is about 500 K with a temperature difference of 100 K between the two ends of the inner tube. The average temperature of the outer tube varying with the position of the mass center is shown in figure 2. The temperature profile of the inner tube is also plotted as a reference. As the outer tube moves toward the cold end, its average temperature decreases gradually, but the outer tube temperature is higher than the

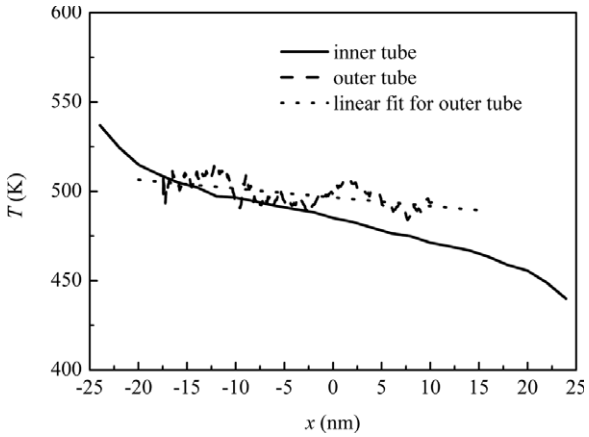

Figure 2. The average temperature of the outer tube varying with the position of the mass center and the temperature profile of the inner tube.

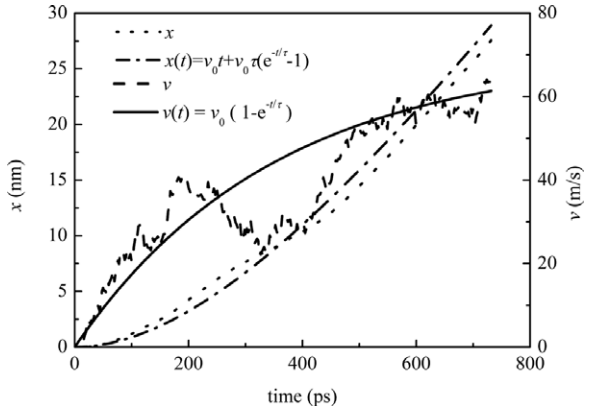

Figure 3. The position and velocity of the outer tube varying with time. For fitting lines, $v_0 = 70$ m s^{-1} and $\tau = 350$ ps.

corresponding local temperature of the inner tube. This is indicative of a thermal local nonequilibrium between the inner and outer tubes during the motion.

The position and velocity of the outer tube as functions of time are plotted in figure 3. Actuated by the temperature gradient, the outer tube speeds up gradually from 0 to about 60 m s^{-1}. This process can be approximately described by the Newton equation for the outer tube

$$m\ddot{x} = F_{\mathrm{T}} - f + N(T), \tag{4}$$

where m is the mass of the outer tube, x is the position of mass center of outer tube, F_{T} is the driving force induced by the thermal gradient, f is the friction, and $N(T)$ is the random force at temperature T. To study the regular motion of the outer tube, we ignore the random force here. Servantie and Gaspard [18] have demonstrated that the friction in DWNTs is proportional to the relative velocity

$$f = \Gamma v, \tag{5}$$

where Γ is the friction coefficient, and v is the relative velocity. Substituting (5) into (4), with the zero initial velocity for the outer tube, we can get

$$v(t) = v_0[1 - \mathrm{e}^{-t/\tau}], \tag{6}$$

where

$$v_0 = F_{\mathrm{T}}/\Gamma, \tag{7}$$

$$\tau = \frac{m}{\Gamma}. \tag{8}$$

Then the position of the mass center can be expressed as

$$x = v_0 t + v_0\tau(\mathrm{e}^{-t/\tau} - 1). \tag{9}$$

The curves of (6) and (9) with $v_0 = 70$ m s^{-1} and $\tau = 350$ ps are shown in figure 3. Although the variation in velocity is large because of the effect of the random force caused by the thermal motion, the position curve fits very well with the simulation result. Based on v_0 and τ, we can estimate the driving force and the friction coefficient. The friction coefficient Γ is about 3.5 amu ps^{-1}, which is on the same order as that calculated by Servantie and Gaspard [19] through molecular dynamics simulations, about 6 amu ps^{-1}. The maximum friction in our simulations is about 0.03 pN/atom. This value is close to that calculated by Guo *et al* [20] (0.085–0.612 pN/atom for three DWNTs), Zhao *et al* [21] (10^{-2}–10^{-5} pN/atom for (5, 0)@(8, 8) DWNTs), and that measured by Cumings and Zettl [2] ($<1.5 \times 10^{-2}$ pN/atom for MWNT). The driving force is consequently estimated to be on the order of pico Newtons.

The final velocity calculated by our simulations is on the same order as those of water droplets or nanoparticles in CNTs simulated by Shiomi and Maruyama [11], Zambrano *et al* [10] and Schoen *et al* [8], respectively, but higher than that measured by Barreiro *et al* [7] in which the velocity is only about 1 μm s^{-1}. The obvious difference between the simulations and the experiments is that the mobile tubes in the experiments by Barreiro *et al* [7] are about 100 times as large as the outer tubes in our simulations. The increase of the system scale cannot increase the magnitude of the driving force (this will be presented in section 3.2 in detail). The low speed in the experiments may arise from the large friction in the experimental systems. The large friction in experiments may be caused by the defects in CNTs that do not exist in the simulations. The gold particles, evaporated on the mobile tubes in experiments, break the symmetry of the CNTs and may also increase the friction.

The efficiency of the nanomachine simulated above in the steady state can be defined as follows

$$\eta = \frac{F_{\mathrm{T}} v_0}{Q}, \tag{10}$$

where Q is the total heat current through the system. For a typical simulation case, e.g. a system with a temperature gradient 2 K nm^{-1}, we can have $Q \sim 10^{-7}$ W, $F_{\mathrm{T}} \sim 10^{-12}$ N and $v \sim 100$ m s^{-1}. Then the efficiency is about 1 ‰. This low efficiency results from the parts of phonon currents that do not interact with the mobile tube strongly. Therefore, increasing the efficiency of such a kind of nanomachine requires selectively exciting some special phonon modes, such

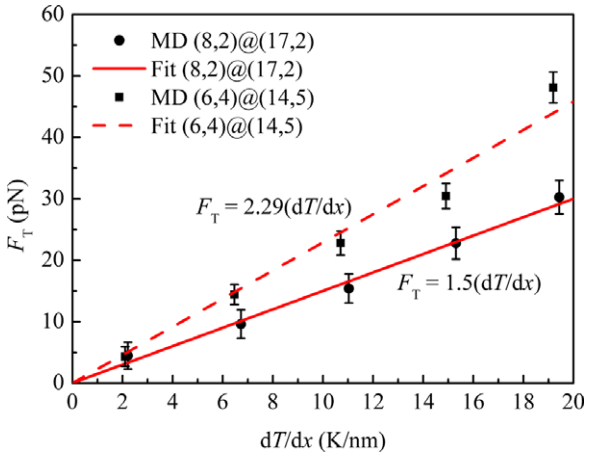

Figure 4. Thermal driving force varying with temperature gradient. The average system temperature is 500 K. For the (8, 2)@(17, 2) DWNT, the lengths of the inner and outer tubes are respectively 13.2 and 2.6 nm. For the (6, 4)@(14, 5) system, the lengths of the inner and outer tubes are respectively 15.1 and 2.5 nm.

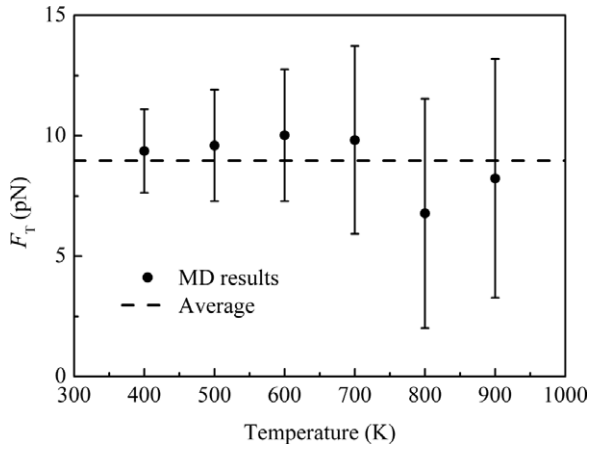

Figure 5. Thermal driving force varying with average system temperature.

as a breathing mode or analogous phonon modes that can interact with the mobile tube.

3.2. Thermal driving force

A (8, 2)@(17, 2) DWNT is typically selected to calculate the thermal driving force since its helical minimum energy track admits the movement of the outer tube along the axis and the slender potential corrugation along the minimum energy track only makes very limited influence on the thermal driving force. A (6, 4)@(14, 5) system is also simulated to mirror the effects of the chirality. The effects of the temperature gradient, chirality pair, system temperature and length of the outer tube on the thermal driving force are considered in our simulations.

Figure 4 gives the driving force as a function of temperature gradient. The magnitude of the thermal driving force varies from several pico Newtons to tens of pico Newtons depending on the temperature gradient. On increasing the thermal gradient, the driving force on the outer tube increases, and an approximate linear relationship can be observed as

$$F_{\mathrm{T}} = \xi \nabla T, \tag{11}$$

where ξ is a proportionality constant. $\xi = 1.5 \times 10^{-21}$ J K^{-1} for the (8, 2)@(17, 2) DWNT and $\xi = 2.29 \times 10^{-21}$ J K^{-1} for the (6, 4)@(14, 5) DWNT. It indicates that the thermal driving force in DWNTs also depends on the chirality pair. Schoen *et al* [8] simulated the thermal driving force of Au particles inside CNTs and also found a linear relationship between the force and the temperature gradient, and the same magnitude of the thermal driving force acted on Au_{775} particles with the similar temperature gradient as in our simulations. Shiomi *et al* [11] simulated the water droplets transport inside a CNT driven by thermal gradient and got a thermal driving force of some pico Newtons with the temperature gradient varying from 0.18 to 1.48 K nm^{-1}. Our simulation data are consistent with those calculated by Schoen *et al* [8] and Shiomi *et al* [11] although the simulated systems are different. Based on (7) and (11), we can also conclude that the final velocity of the outer tube is approximately proportional to the thermal gradient of the inner tube.

The thermal driving force in the (8, 2)@(17, 2) DWNT varying with the system temperature is shown in figure 5 with the temperature difference between the two ends of the inner tube being kept at 120 K (the temperature gradient is about 6.8 K nm^{-1}). As the temperature increases from 400 to 900 K, the thermal driving force does not change much, and only fluctuates near an average value about 9 pN. This insensitivity to the temperature is different from the thermophoresis in fluids where the thermophoretic force decreases with increasing temperature [22]. Although the system temperatures are different, about 0.31×10^{-6}–0.39×10^{-6} W, the heat currents nearly remain unchanged because of the same temperature gradient. From this point of view, the thermal driving force may be controlled by the heat flux. Although the driving force is not sensitive to the temperature, the friction will increase as the temperature increases. So, based on (7), the final velocity of the outer tube will decrease at a higher temperature.

The thermal driving force in the (8, 2)@(17, 2) DWNT at 500 K as a function of the outer tube length is shown in figure 6. Two configurations with lengths of the inner tubes respectively 19.8 and 13.2 nm are simulated. The temperature differences between the two ends of the inner tube for the two systems are 200 and 120 K. The thermal driving force in the system with a longer inner tube is larger than that with a shorter inner tube. This maybe results from the lower restriction of phonon transport and the larger thermal gradient in the longer inner tube system. As the length of the outer tube is less than 5 nm, the force decreases with the reduction of the tube length. However, as the length is larger than 5 nm, the thermal driving force is nearly constant. We find that the temperature profiles of the inner tube do not change on varying the length of the outer tube, as shown in figure 7. It indicates that the outer tube length does not affect the heat conduction through the DWNTs seriously, and the thermal driving force usually remains constant.

The physical mechanism of the thermal gradient induced actuation can be understood by considering the drag on the

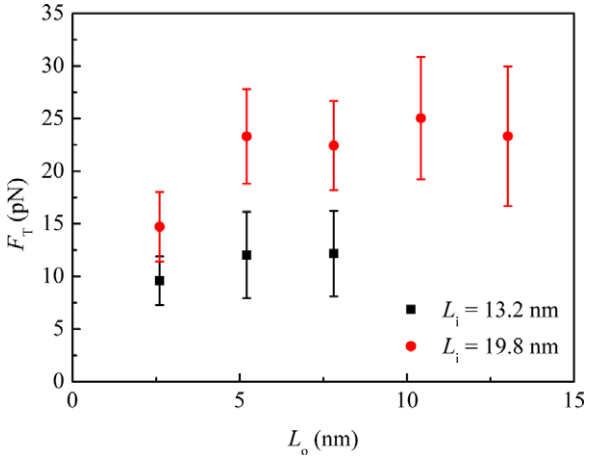

Figure 6. Thermal driving force varying with length of the outer tube.

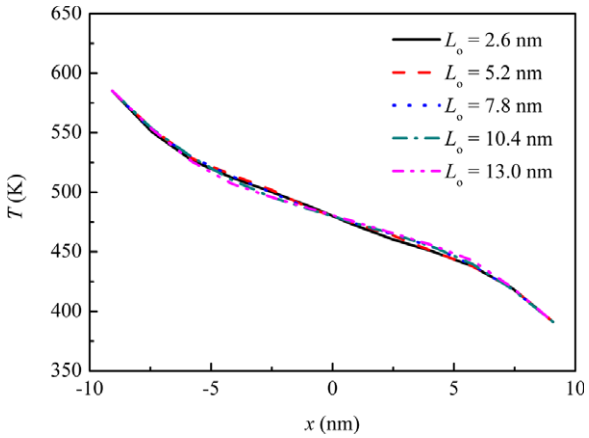

Figure 7. Temperature profiles in the 19.8 nm inner tube for different outer tube lengths.

outer tube of the phonon current [7, 23]. In more detail, that the thermal driving force is not affected by the length of the outer tube implies that the thermal driving force acts only on the area near the edges of the outer tube. The breathing mode phonons were considered responsible for the thermally driven motion in CNTs [9, 24]. When the phonons of breathing mode translate from one end to the other in the inner tube, they collide with the outer tube, interact with the outer tube, lose their momentum and transfer it to the outer tube. If the outer tube is long enough, the phonons have enough time to interact with the outer tube, and transfer all their momentum to the outer tube. In this case, the increase of the outer tube length will not increase the thermal driving force because the phonon current is constant in the inner tube. When the outer tube is too short, however, the phonons have insufficient time to interact with the outer tube, and only transfer part of their momentum. As a result, the shorter the outer tube length, the smaller momentum the phonons transfer. Consequently, the thermal driving force will decrease with a decrease of the outer tube length.

3.3. Motion trace and controllability

DWNTs have various structures according to the chirality pairs. Saito *et al* [14] studied the interwall potentials of

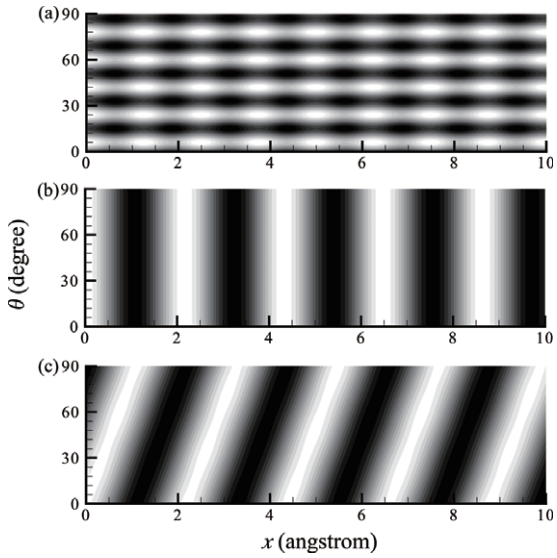

Figure 8. Interwall potential patterns for DWNTs with different chirality pairs: (a) (5, 5)@(10, 10), (b) (13, 0)@(22, 0), (c) (8, 2)@(17, 2).

Table 1. Structural parameters of three DWNTs.

Case	Chirality pair	Length (nm)	Radius (nm)	Interwall distance (nm)
1	(5, 5)@(10, 10)	24.9/7.5	0.344/0.688	0.344
2	(13, 0)@(22, 0)	25.9/5.2	0.516/0.873	0.357
3	(8, 2)@ (17, 2)	26.4/5.2	0.364/0.718	0.354

DWNTs for a variety of sets of inner and outer nanotube chiralities. The potential patterns were found to depend sensitively on the chirality pairs. A classification scheme of DWNTs according to their symmetries was then proposed in more detail by Lozovik *et al* [25, 26]. It is apparent that the potential pattern, or the structure, will affect the relative motion of DWNTs attached to a thermal gradient.

To identify how the potential pattern affects the thermal gradient driven motion, trace and controllability, in DWNTs, three DWNTs with different chirality pairs are simulated as tabulated in table 1. The interwall distance in all the systems is about 0.34 nm, which ensures the stability of the structure and movement. The potential patterns of the three DWNT systems are plotted in figure 8. The two degrees of freedom of motion are taken to be sliding along the nanotube axis and rotation around the nanotube axis. A darker color denotes a lower potential energy. Allowing for the difference in DWNTs' lengths, the potential patterns calculated in this paper are quantitatively in agreement with the results in [14] and [25]. If the outer tube is completely released, it will fall into the potential valleys with the lowest energy. Driven by a small force, it will choose an easy way, which is just the minimum energy track, to move. The minimum energy tracks of the (5, 5)@(10, 10), (13, 0)@(22, 0) and (8, 2)@(17, 2) DWNTs are along the tube axis, circumference and helix, respectively, as illustrated in figure 8. Between two neighbor minimum energy tracks is a potential barriers ΔU, which is the restriction on the ability from changing tracks for the outer tube. The barriers of

case 1, 2 and 3 in our simulations are 0.024 eV, 0.15 eV and 0.12 eV, respectively.

With the two ends of the inner tube being at 600 and 400 K, the outer tube will speed up. The position of the CoM and the rotation angle along the circumference of the outer tube varying with time are shown in figure 9. Driven by the temperature difference, the outer tubes of all the three DWNTs move towards the specific directions. For the (5, 5)@(10, 10) DWNT as shown in figure 9(a), the outer tube translates along the axis and oscillates in the circumferential direction. The maximum oscillation amplitude is about 15°, less than the separation angle between two neighbor minimum energy tracks in the (5, 5)@(10, 10) DWNT. It indicates that the movement of the outer tube is confined in the minimum energy tracks as shown in figure 8(a). The same conclusion can be drawn for the (13, 0)@(22, 0) DWNT (figure 9(b)) in which the outer tube rotates around the axis with very small oscillations in the axis direction (less than 0.06 nm). In this case, however, we should point out that because of the perpendicularity between the minimum energy track and the thermal driving force, the rotation direction of the outer tube, that is clockwise or anticlockwise, depends on the initial actuation. The minimum energy track in the (8, 2)@(17, 2) DWNT has been demonstrated to be a helix above. For this DWNT, figure 9(c) shows the trace of the outer tube, and the inset gives the rotation angle as a function of the translational distance in a polar coordinate system. The rotational angle is proportional to the translational distance, indicative of a helix trace. The helix angle of the trace is $810° \pm 9.8°$ nm^{-1}, which agrees with the helix angle of the minimum energy tracks, 829° nm^{-1} obtained by figure 8(c). The small deviation may arise from the deformation of the tubes at different temperatures. Therefore, the motion in this system is also consistent with the minimum energy tracks. Under the current conditions, the thermally driven DWNTs run along the minimum energy tracks with specific directions depending on the DWNT chirality pairs. From this point of view, the directional control of DWNTs based nanodevices can be realized.

The minimum energy track cannot always confine the trace of the outer tube. Two important factors should be considered, i.e., temperature and potential barrier, respectively. Imaging the outer tube as a 'large particle', and the motion of the outer tube along and around the inner tube as the motion of the 'large particle' in a regular two-dimensional potential field. The 'regular' here means that the potential contour lines in the field are straight lines and parallel to each other. According to the energy equipartition theorem, each degree of freedom of the particle has a kinetic energy $k_{\mathrm{B}}T/2$ (k_{B} is the Boltzmann constant). If this energy is less than the potential barrier ΔU, the particle will be confined in a potential valley. However, if the kinetic energy is larger than the barrier, the particle is able to jump from one potential valley to another. According to the potential barrier ΔU, we can define a critical temperature

$$T_{\mathrm{c}} = \sqrt{2\Delta U/k_{\mathrm{B}}}, \tag{12}$$

which determines whether the motion is along the minimum energy track or not.

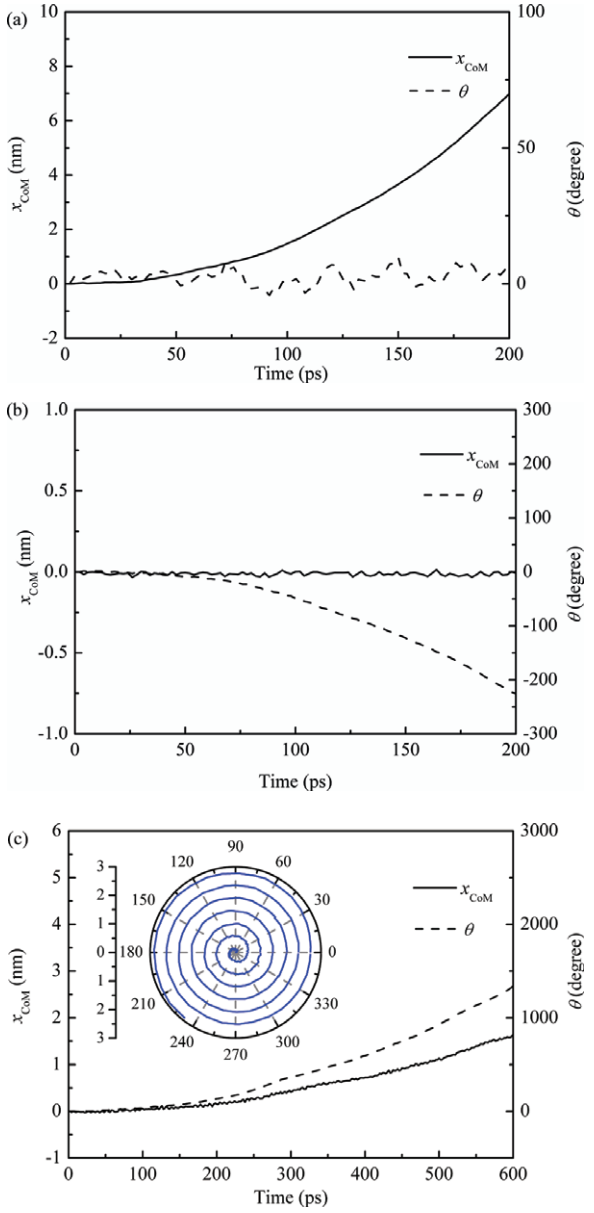

Figure 9. The position of center of mass and the rotation angle of the outer tube varying with time for: (a) (5, 5)@(10, 10), (b) (13, 0)@(22, 0), (c) (8, 2)@(17, 2). The average temperatures of the simulation systems are 500 K with the two ends of the inner tube being at 600 and 400 K. The inset in (c) plots the trace of the motion in a polar coordinate system whose polar axis and angle units are nanometers and degrees, respectively.

In the discussion above, we have only considered the situation in which the particle is actuated by random thermal motion. In thermal gradient driven motion, the outer tube is also under the action of a driving force which is a macroscopic force opposite the direction of the thermal gradient. The macroscopic kinetic energies of the outer tubes are also found to be larger than the potential barriers in some situations. However, the analysis above can still be useful in these situations. Under the action of the driving force, the outer tube will reach a very large kinetic energy, but the motion is generally perpendicular to the potential gradient. So it can not be used to overcome the potential barrier.

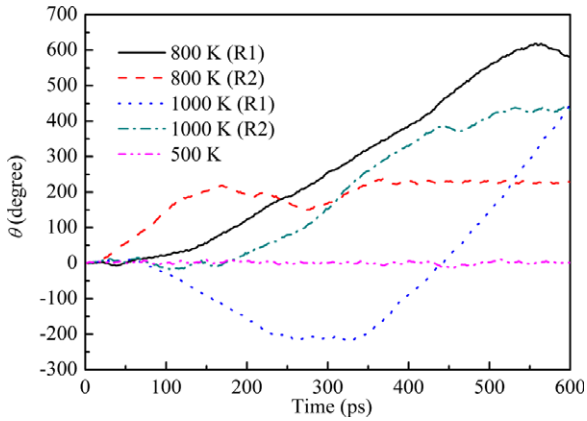

Figure 10. The rotation angle of the outer tube in the (5, 5)@(10, 10) DWNT varying with time. The average temperature is 800 or 1000 K and the temperature difference is 200 K. We run twice for each average temperature, marked by R1 and R2.

For the three DWNTs simulated above, the critical temperatures are 557 K, 3478 K and 2783 K, respectively. Since the average system temperature, 500 K, is less than the critical temperatures, the motion of the outer tubes can be confined in the minimum energy tracks. For the (5, 5)@(10, 10) DWNT, since the system temperature is very close to the critical temperature, obvious oscillations in the circumferential direction can be observed, as shown in figure 9(a). Additional MD simulations, setting the system average temperatures of the (5, 5)@(10, 10) DWNT at 800 and 1000 K with a temperature difference of 200 K, are performed. We run twice for each average temperature. For all cases, the outer tubes are found to move towards the cold ends, as observed above. However, the motions in the circumferential direction are quite different. Figure 10 shows the rotational angle as a function of time. At 800 and 1000 K, the outer tube can rotate clockwise or anticlockwise, even change rotational directions during the motion. The random behaviors imply that the outer tubes are not confined in the minimum energy tracks. Similar behavior was also observed in the (7, 7)@(21, 0) nano-oscillators [27], in which the inner tube of an isothermal DWNT can get across the potential barriers very easily since the critical temperature is estimated to be only about 60 K according to the potential barrier against the axial sliding.

The critical temperature serves as a crucial criterion for the directional control of motion of DWNTs or MWNTs. To confine the relative motion in the minimum energy tracks, the temperature of the system should be lower than the critical temperature defined by the potential barrier between two neighbor potential valleys. The higher the critical temperature is, the better direction controllability the system has. In order to realize the precise control of the motion, a high potential barrier is required. We should note that the potential barrier of DWNT is not only dependent on the chirality pairs of DWNT, but also on the contact area of the two tubes, $\Delta U = \Delta U(S)$ where S is the contact area. For commensurate DWNTs, the potential barrier is proportional to the length of the contact surface, which means $\Delta U(\alpha S) = \alpha \Delta U(S)$ where α is a scale factor, so we can increase the potential barrier by increasing the length of the tubes. For incommensurate DWNTs, the potential barrier is an approximate periodic function of the contact area, and it only fluctuates near an average value when the tube length increases [25]. In this case, chirality pairs with large potential barriers and high critical temperatures are preferable for trace control in practice.

4. Conclusion

Using molecular dynamics simulations, we have studied the thermal gradient induced actuation in DWNTs. The simulation results indicate that the thermal gradient can be used to drive the relative motion of DWNTs, and the final velocity of the relative motion can be on the order of 100 m s^{-1}. The thermal driving force is on the order of pico Newtons when the temperature gradient is about 1 K nm^{-1}. The driving force is approximately proportional to the temperature gradient, but not sensitive to the system temperature. When the length of outer tube is shorter than 5 nm, the driving force decreases with decreasing outer tube length. As the length of outer tube is longer than 5 nm, the thermal driving force is nearly constant. This can be explained by the phonon collisions with the outer tube. When the length of the outer tube is long enough, the phonons of the breathing mode hit the outer tube and lose all their momentum. If the outer tube is too short, the phonons can not completely interact with the outer tube, and only part of their momentum is lost. A critical temperature can be defined by the potential barrier of DWNTs perpendicular to the minimum energy track of the potential patterns between two walls. When the system temperature is higher than the critical temperature, the motion shows random behavior. When the system temperature is lower than the critical temperature, the motion, translational and/or rotational, is confined within the minimum energy track, which is indicative of directional control. This may be useful for the design of thermally actuated nanodevices based on CNTs.

Acknowledgment

This work has been supported by the National Natural Science Foundation of China Grant 50606018 and the Tsinghua National Laboratory for Information Science and Technology (TNList) Cross-discipline Foundation.

References

[1] Iijima S 1991 *Nature* **354** 56–8
[2] Cumings J and Zettl A 2000 *Science* **289** 602–4
[3] Forro L 2000 *Science* **289** 560–1
[4] Tuzun R E, Noid D W and Sumpter B G 1995 *Nanotechnology* **6** 52–63
[5] Srivastava D 1997 *Nanotechnology* **8** 186–92
[6] Zheng Q S and Jiang Q 2002 *Phys. Rev. Lett.* **88** 45503
[7] Barreiro A, Rurali R, Hernandez E R, Moser J, Pichler T, Forro L and Bachtold A 2008 *Science* **320** 775–8
[8] Schoen P A E, Walther J H, Arcidiacono S, Poulikakos D and Koumoutsakos P 2006 *Nano Lett.* **6** 1910–7
[9] Schoen P A E, Walther J H, Poulikakos D and Koumoutsakos P 2007 *Appl. Phys. Lett.* **90** 253116

[10] Zambrano H A, Walther J H, Koumoutsakos P and Sbalzarini I F 2009 *Nano Lett.* **9** 66–71
[11] Shiomi J and Maruyama S 2009 *Nanotechnology* **20** 55708
[12] Allen M P and Tildesley D J 1987 *Computer Simulation of Liquids* (Oxford: Clarendon)
[13] Brenner D W 1990 *Phys. Rev.* B **42** 9458–71
[14] Saito R, Matsuo R, Kimura T, Dresselhaus G and Dresselhaus M S 2001 *Chem. Phys. Lett.* **348** 187–93
[15] Galliero G and Volz S 2008 *J. Chem. Phys.* **128** 64505
[16] Maruyama S 2002 *Physica* B **323** 193–5
[17] Pop E, Mann D, Wang Q, Goodson K and Dai H J 2006 *Nano Lett.* **6** 96–100
[18] Servantie J and Gaspard P 2003 *Phys. Rev. Lett.* **91** 185503
[19] Servantie J and Gaspard P 2006 *Phys. Rev.* B **73** 125428
[20] Guo W L, Guo Y F, Gao H J, Zheng Q S and Zhong W Y 2003 *Phys. Rev. Lett.* **91** 125501
[21] Zhao Y, Ma C C, Chen G H and Jiang Q 2003 *Phys. Rev. Lett.* **91** 175504
[22] Talbot L, Cheng R K, Schefer R W and Willis D R 1980 *J. Fluid Mech.* **101** 737–58
[23] Cao B Y and Guo Z Y 2007 *J. Appl. Phys.* **102** 53503
[24] Burghard M 2008 *Angew. Chem. Int. Edn* **47** 8565–6
[25] Lozovik Y E, Minogin A and Popov A M 2003 *Phys. Lett.* A **313** 112–21
[26] Belikov A V, Lozovik Y E, Nikolaev A G and Popov A M 2004 *Chem. Phys. Lett.* **385** 72–8
[27] Xu Z P, Zheng Q S and Chen G H 2007 *Phys. Rev.* B **75** 195445